Segmentation and Kinetic Analysis of Breast Lesions in DCE-MR Imaging using ICA

Sebastian Goebl*[1], Anke Meyer-Baese[2], Marc Lobbes[3], and Claudia Plant[4,5]

[1] University of Munich, Germany, goebl@dbs.ifi.lmu.de
[2] Florida State University, Tallahassee, USA, ameyerbaese@fsu.edu
[3] Maastricht University Medical Center, The Netherlands, marc.lobbes@mumc.nl
[4] Helmholtz Zentrum München, Germany, claudia.plant@helmholtz-muenchen.de
[5] Technische Universität München, Germany

Abstract. Dynamic Contrast Enhance-Magnetic Resonance Imaging (DCE-MRI) has proved to be a useful tool for diagnosing mass-like breast cancer. For non-mass-like lesions, however, no methods applied on DCE-MRI have shown satisfying results so far. The present paper uses the Independent Component Analysis (ICA) to extract tumor enhancement curves which are more exact than manually or automatically chosen regions of interest (ROIs). By analysing the different tissue types contained in the voxels of the MR image, we can filter out noise and define lesion related enhancement curves. These curves allow a better classification than ROI or segmentation methods. This is illustrated by extracting features from MRI cases and determining the malignancy or benignity by support vector machines (SVMs). Next to this classification by kinetic analysis, ICA is also used to segment tumorous regions. Unlike in standard segmentation methods, we do not regard voxels as a whole but instead focus our analysis on the actual tissue types, and filter out noise. Combining all these achievements we present a complete workflow for classification of malignant and benign lesions providing helpful support for the fight against breast cancer.

Keywords: Breast DCE-MRI, Independent component analysis, Breast lesion segmentation

1 Introduction

To run a chance of surviving breast cancer it is uttermost important to discover malignant tumors at an early stage. Deaths by breast cancer are highly reduced by early treatment. In his fundamental publication "Signs In MR-Mammography" Werner A. Kaiser states: "If we had a diagnostic method that enabled us to detect and remove all breast cancers 5 to 10 mm in size, we could practically eliminate breast cancer deaths" [12]. Methods able to diagnose even very small lesions play an important role in the fight against breast cancer. Dynamic Contrast Enhanced-Magnetic Resonance Imaging (DCE-MRI) is a very useful tool

* Corresponding author.

for such methods. It allows analyzing tissue by reference to blood flow. Enhancement curves representing the change in blood flow are obtained from DCE-MRI and help to differentiate between malignant and benign lesions. Research has demonstrated the high relevance of enhancement curves for mass-like lesions [17,11]. However, this method has not yet proven successful for the assessment of non-mass-like lesions [10]. This may be due to the fact that it is common use to obtain an enhancement curve from the mean enhancement of a selected area, the region of interest (ROI). However, the chosen ROI is taken from an area inside the lesion that shows the strongest enhancement. There might be cases where it does not sufficiently represent the whole lesion. This is especially relevant for non-mass-like lesions which show a very diffuse structure that is hard to separate from normal body tissue. Instead, mass-like lesions show a compact, mass-like structure, hence the name. The disadvantages of the standard ROI selection represent the main motivation for applying the independent component analysis (ICA) to enhancement curves obtained from DCE-MRI. The goal is to extract curves that represent different tissue structures and, thus, to obtain tumor curves that represent tumorous tissue better than a manually selected ROI or automatic segmentation. MRI voxels represent 3-dimensional cubes of different tissue types. ICA allows to differentiate various tissue types in a single MRI voxel. Overall, the application of ICA on DCE-MRI refines the extraction of enhancement curves. Thus, it is able to achieve better results than using standard ROI or segmentation methods, which leads to superior results.

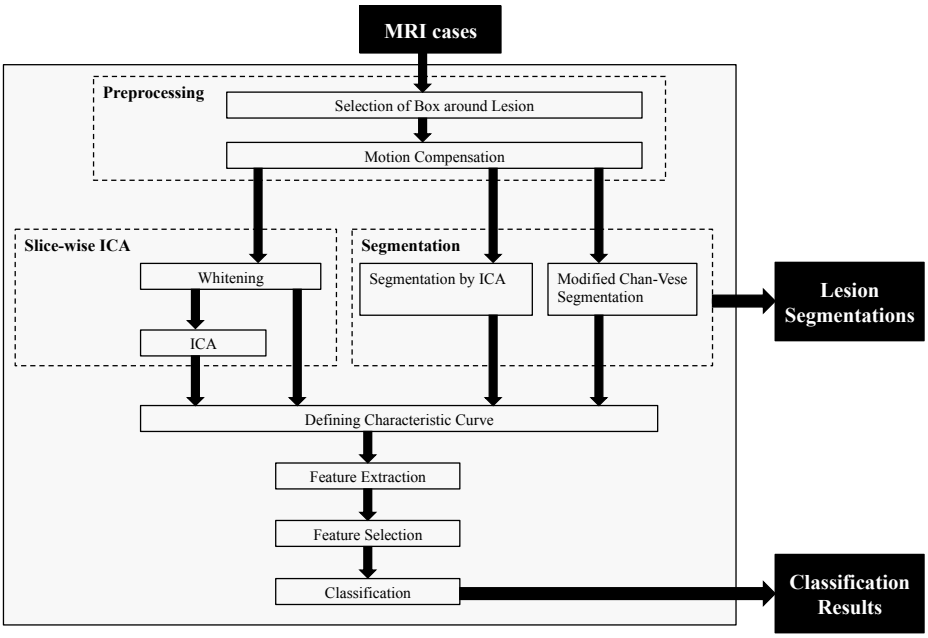

Fig. 1: Workflow of MR image processing.

1.1 Contribution

In recent work [5,6] we approximated extracted tumor curves to an empirical mathematical model based on the phenomenological universalities (PUN)[4] showing its profit to lesion classification. Tying on this work, we now present a complete workflow (Figure 1) for classification of malignant and benign non-mass-like as well as mass-like lesions using ICA. For given MR images our proposed method outputs classification results despite hard to outline non-mass-like lesions. Noise gets filtered out of the enhancement curves, tumor-related curves are detected. Also, the proposed method allows to automatically segment tumor regions and even is able to handle MRI images obtained by a very small number of time points. This renders it possible to process MRI images with a very high resolution and, thus, very little time points, but having the advantage of finding even very small lesions. Furthermore, features will be extracted for classification by support vector machines (SVMs). Our method will be evaluated using 80 MRI cases containing malignant and benign lesions. Our workflow includes a segmentation method unrelated to ICA, allowing an evaluation of the benefits of using ICA. All cases we present are provided and recorded by the Maastricht University Medical Center following the MRI protocol stated in Table 1.

Contrast agent:	gadopentetate dimeglumine
Dose (mmol/kg):	.1
Injection rate (ml/s):	2, followed by saline flush
Field strength (Tesla):	1.5
Pulse sequence:	T1w 3D FLASH
Scan coverage:	bilateral
Plan:	transverse
Flip (degrees):	10
FOV:	280 x 338 x 150
Matrix:	352 reconstructed
Reconstructed voxel size (mm):	1
Slice thickness (mm):	1
Slices:	150, no overcontiguous slices
Volume scan time (min):	1.4
Dynamic acquisition time (min):	1.4, 2.8, 4.2, 5.6

Table 1: MRI protocol parameters.

2 Related Work

Several approaches have been made to identify malignant and benign breast lesions by analyzing the results obtained by DCE-MRI. Mainly tissue enhancement curves and shape or texture properties have been extracted as distinctive features. Work on enhancement curves provided the best results and is outlined in this section. Newell et al. [17] extracted kinetic features (in addition to shape and texture features) from breast DCE-MRI cases and trained a classifier to predict lesion quality. Kinetic features were obtained from a manually chosen ROI, a mean signal was calculated from the most enhancing part of the ROI and two parameters were extracted: uptake (i.e. how fast the contrast agent is been taken up by tissue) and washout rate (i.e. how fast the contrast agent disappears due to following blood containing no contrast agent any more). The results

where evaluated by a receiver operating characteristic (ROC) which showed an area under the curve (AUC) of .88 for mass-like lesions, but for non-mass-like lesions only a AUC of .59, hardly better than the random decision of an AUC of .5. Another approach is done by Jansen et al. [11]. They extracted and analyzed qualitative and quantitative features from DCE-MRI enhancement curves for mass-like, non-mass-like and focus enhancements. All features were obtained from a manually selected ROI. As qualitative features initial rise and delayed phase of the enhancement curve were defined by a specialist. Additionally, several quantitative features were calculated. The diagnostic performance is examined for each single quantitative feature, and evaluated using ROC. For mass-like lesions the AUC reaches up to .75. However, for non-mass-like lesions the best feature reaches only an AUC of .67. For focus enhancements (being only 7% of all cases) there has been a best AUC of .53. The disadvantage of determining the ROI manually is especially large, if the lesion is very heterogeneous and hard to outline manually. This is rather the case for non-mass-like than for mass-like lesions. To avoid this problem the manual step has to be excluded. Therefore, two ways to proceed are possible. One could either find a method to outline the ROI automatically. This direction was chosen by Stoutjesdijk et al. [19] by determining the ROI using mean shift multidimensional clustering (MS-MDC). However, they only achieved a result as good as with a specialist chosen ROI, but did not outperform him. Also semi-automatic lesion extraction is performed by threshold based segmentation. Hoffmann et al. [8] proposed a modification for the segmentation algorithm by Chan and Vese [2]. As comparison algorithm this method is included in our proposed workflow. The other way possible is to use a method to analyze lesion kinetics without determining a ROI. Extraction of different enhancement curves due to differently enhancing tissue types has first been done for functional MRI. McKeown et al. [15,16] have applied blind source separation techniques on functional brain MR images. Due to the MRI technology, with a higher resolution less time points can be measured. Therefore, many breast MRI protocols only have a very small number of measured time points. The number of unmixed signals in ICA can not exceed the number of measured signals which equals the number of measured time points. This results in the lack of a high number of signals being able to be obtained from ICA. Koh et al. [13] avoided this problem of a lack of time points by using a protocol of 65 time points in their feasibility study. They produced clear results and could outline the tumor component in the visualization of mostly a single extracted signal component. However, this approach can only been seen as preliminary work, for it is lacking the chance of realistic usability since such a high number of measured time points results in a resolution far too low to be sufficient for breast lesion detection. Nonetheless, we stressed the importance of identifying already very small lesions, which needs a higher resolution. To fill this gap, we propose a combination of ICA, segmentation and kinetic analysis that yields proven results for high resolution MRIs of $1mm$ slice thickness.

3 Segmentation and Kinetic Analysis using ICA

Our aim is to provide a complete workflow for segmentation and kinetic analysis using ICA. The workflow covers all pre-processing steps and results in a segmentation and in classification results. Before introducing each step of the workflow, we first introduce our application of ICA on DCE-MR images, since this is fundamental for both segmentation and kinetic analysis.

3.1 ICA on DCE-MRI

Independent Component Analysis The method of Independent Component Analysis (ICA) has been developed by Hyvärinen and Oja [9] for the problem of blind source separation for the task of unmixing signals into independent single signals. We apply ICA on DCE-MR imaging, which opens up several opportunities for analyzing MR images. As mentioned in Section 2, the ROI method uses only a few voxels in order to obtain a tumor enhancement curve. The tumor might not be represented by this exactly enough for further analysis. Furthermore, a ROI needs to be drawn by an expert for every single case and depends on the expert's knowledge. The basic idea of ICA on DCE-MRI is that not every voxel shows an enhancement curve, but every tissue type has a typical enhancement curve that sheds light on its quality, whether it is malignant lesion tissue, benign lesion tissue or a completely other tissue type. The application of a ROI selects only several voxels, neglecting tissue types and unselected voxels. It is creating voxel enhancement curves that actually are mixtures of enhancement curves of all tissue types combined in the voxels. Enhancement curves achieved this way only show the approximate enhancement of lesion tissue. In the MRI protocol used for the cases discussed in this work, the voxel volume is $1mm^3$. So it is very likely that voxels are containing different tissue types at the same time.

The total signal intensity of a voxel is the sum of the intensities that every tissue type in this voxel emits. Here, ICA unmixes the different tissue types out of this mixture. Like ICA is calculating original signals and a mixing matrix, ICA on DCE-MRI reconstructs the original tissue types and how they are mixed together in each voxel. As result we gain enhancement curves for each tissue type. Principally, there are two ways to apply ICA on DCE-MRI: temporal [14] and spatial [15,14] ICA. The temporal approach is the most intuitive: Every voxel changes its enhancement or signal intensity over time: for every pre- and post-contrast time point it shows a value. These signals are unmixed by ICA. However, this means that a very high number of signals showing very few time points needs to be unmixed. Already for an area of 25×25 voxels this would result in 625 single signals each showing only 5 time points, as for our MRI protocol. Thus, it did not prove successful to extract meaningful unmixed enhancement curves by temporal ICA. The other way we adopt to apply ICA on DCE-MRI is spatial ICA. We derive this method from original ICA, where m mixed signals $\mathbf{x} = (x_m)$ are composed by a matrix of mixing coefficients $A = (a_{mn})$ and n independent random variables $\mathbf{s} = (s_n)$, such that $\mathbf{x} = A\mathbf{s}$. The solution to unmixing the

mixed variables equally is $\mathbf{s} = W\mathbf{x}$ with $W = A^{-1}$. There are restrictions to ICA: since the signals are calculated by maximizing the mutual independence, the may not be correlated. Otherwise, ICA would maximize their independence and create signals less similar to the correlated signals. Also, ICA can not create more unmixed signals than the number of observed signals, i.e. $n \leq m$.

Independent Component Analysis on Dynamic Contrast Enhanced-Magnetic Resonance Imaging Different tissue types show different enhancement curves. Parts of the lesion may enhance differently as well as non-lesion related tissue types and noise. Since a MRI voxel may include more than one tissue type, it is important to separate these overlaid areas and enhancement curves in order to obtain the original curves and lesions without noise. Spatial ICA calculates these variously enhancing curves and how each voxel is influenced by which enhancement curve. We derive spatial ICA on DCE-MRI from the original ICA definition and set $\mathbf{x}$ in equation $\mathbf{x} = A\mathbf{s}$ so that $x_1, \ldots, x_m$ describe a slice of the m-th subtraction MR images that are obtained by subtracting the pre-contrast MR image from the m-th MR image. This results in the pre-contrast subtraction image showing zero enhancement and the following post-contrast subtraction images showing an enhancement relative to the pre-contrast subtraction image. They are denoted as subtraction images 1 to m. Since the 1st subtraction image is defined as the pre-contrast image subtracted by the pre-contrast image, it contains no additional information. The following definitions can be applied to pre- and post-contrast images without subtraction. However, since subtraction images are used more often by related work and provided better results here as well, we define ICA on DCE-MRI for subtraction images, but without loss of generality. Also, we process the MR images slice per slice. It is also possible to apply ICA on all slices at once, but too many differently enhancing tissues produce no clear result. Every subtraction image x_i consists of v voxels, so that a voxel j of a subtraction image x_i is denoted by x_{ij}. For easier notation we change our ICA equation to $X = AS$. Thus, we derive $X = \begin{pmatrix} \mathbf{x}_1 \\ \vdots \\ \mathbf{x}_m \end{pmatrix} = \begin{pmatrix} x_{11} & \cdots & x_{1v} \\ \vdots & \ddots & \vdots \\ x_{m1} & \cdots & x_{mv} \end{pmatrix}$. This is the MR image series obtained from the scanner. The idea of spatial ICA on DCE-MRI is that the signal intensity of every voxel is build by the sum of all the signal intensities of the tissue types it is containing. Objective of ICA on DCE-MRI is to unmix the enhancement of every voxel into the amount of enhancement that is caused by every single tissue type included in the voxel. The signals $\mathbf{s}$ are these different tissue types. Here $\mathbf{s}$ defines for every tissue type how it affects each voxel. The mixing matrix M then defines how every voxel on every subtraction image is affected by every tissue type. Thus, we define $S = \begin{pmatrix} \mathbf{s}_1 \\ \vdots \\ \mathbf{s}_n \end{pmatrix} = \begin{pmatrix} s_{11} & \cdots & s_{1v} \\ \vdots & \ddots & \vdots \\ s_{n1} & \cdots & s_{nv} \end{pmatrix}$, where n denotes the number of signals and v the number of voxels. A signal here is also called an

independent component (IC). So, s_{kj} denotes the j-th voxel on the k-th independent component. Finally, we define the mixing matrix $A = \begin{pmatrix} a_{11} & \cdots & a_{1n} \\ \vdots & \ddots & \vdots \\ a_{m1} & \cdots & a_{mn} \end{pmatrix}$, with m denoting the number of subtraction images and n the number of signal or ICs. Every a_{ik} denotes the mixing coefficient for the k-th IC on the i-th subtraction image. An informal, more intuitive description is that the mixing matrix A puts together every subtraction image out of each independent component by weighting it by its coefficient.

The tissue types equal the independent components (ICs) that have been extracted by ICA. Thus, the enhancement curves for every tissue type k are represented by $(a_{0k}, a_{1k}, \ldots, a_{mk})$ where m denotes the number of subtraction images. For every tissue type respectively for every IC, A shows how much each voxel is represented by this tissue type. This allows a graphical view on every tissue type, which will be used for segmentation by ICA.

Application on Malignant Lesion An example demonstrates our method. Its MRI subtraction image time series is shown in Figure 2. The first subtraction image shows $mri_2 - mri_1$ (The actual first subtraction image $mri_1 - mri_1$, of course, contains no information). A rectangular area only containing the lesion and its direct neighborhood has been cut out and motion compensated as explained in the following workflow description. Judged by eye, the overall enhancement increases from Figure 2a to 2d, but apart from that, an inner separation of components can hardly be drawn. The Figures 3a to 3d show the

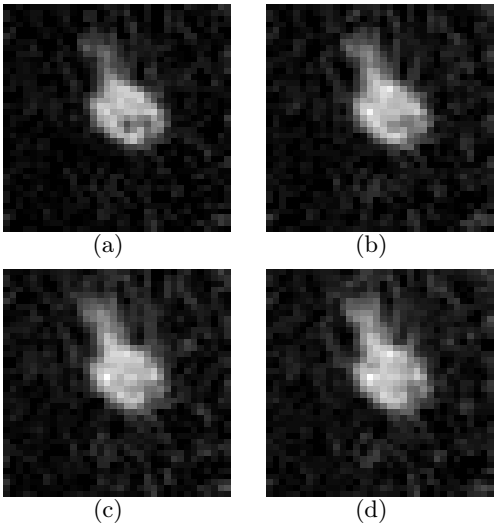

Fig. 2: Subtraction images 1 to 4 of malignant lesion.

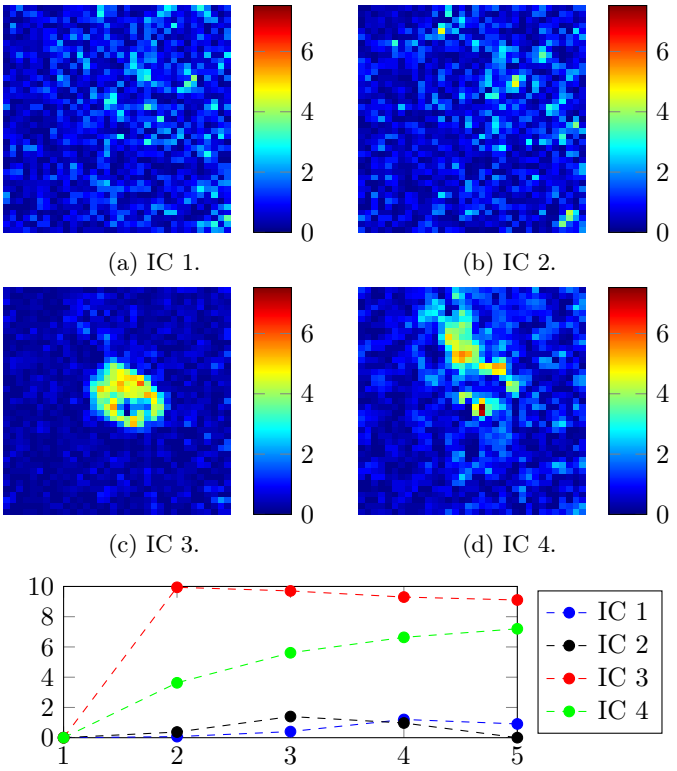

(a) IC 1. (b) IC 2.

(c) IC 3. (d) IC 4.

(e) Mixing matrix A.

Fig. 3: Estimated independent components and visualization of mixing matrix A of malignant lesion.

four estimated independent components, while Figure 3e visualizes the mixing matrix A by showing the curves corresponding to the portion of each IC to each subtraction image. For easier visibility of the voxel intensities a blue to red color map has been applied. As already mentioned the independent components are normalized to unit variance (whitening step). The product of voxel intensity and signal enhancement as shown in matrix A is invariant. However, the visualization of the independent components already allows an interpretation of the results. IC 1 and 2 obviously contain noise which is widespread with no enhancement concentrations. Also it is showing only few higher voxel intensities. That, together with the low and indifferent enhancement curves of matrix A, allows an identification as noise. On the contrary, IC 3 and 4 show a concentration in the enhancement of their voxels. They also show higher intensities both in the IC visualizations and their enhancement curves of matrix A. While IC 3 shows a compact round shape, IC 4 enhances with a less exact contour. Also the enhancement curves show a clearly different behaviour. IC 3 enhances very strongly in the beginning, slighly decreasing in the following subtraction images.

On the other hand, IC 4 continues enhancing up to the last subtraction images, but at a slower pace. Due to the idea of ICA on DCE-MRI we can assume that IC 3 and 4 consist of different tissue types.

3.2 Workflow for Segmentation and Kinetic Analysis

In the last section we have shown how ICA is applied on DCE-MR images. It presents the core technique for the our MR image processing workflow. In this section all processing steps are depicted. A general view has already been presented on Figure 1.

Preprocessing Before applying our methods on the MR images the data is preprocessed. The relevant region where a radiologist locates the lesion is cut out in a box of cubical shape, assuring that all tumorous tissue lies inside the area. For this area a non-rigid motion compensation algorithm based on the approach of Brox [1] is employed. The parameters of the motion compensation algorithm are chosen in the following way: smoothness term $\alpha = 100.0$, regularization parameter $\gamma = 10.0$ and the refinement factor $\eta = .8$. Additionally presmoothing by convolving each image with a Gaussian with standard deviation $\sigma = .6$ is performed. Finally, the transverse slices of the cut out box are selected for the further analyzing steps.

Segmentation Two aspects motivate the development of a method for lesion segmentation. First, knowledge about the contours of the lesion is crucial for surgery. Only an exact segmentation allows the surgeon to remove all tumorous tissue without missing cancer cells that will continue growing with possibly deadly consequences. Knowing the exact boundaries of the lesion also prevents removing too much healthy breast tissue and helps avoiding a mastectomy. Second, for extracting kinetic features it is compulsive to know which voxels belong to the lesion itself and which belong to the surrounding area. Only then, features like the mean intensity of all tumor voxels can be calculated correctly. For the final evaluation of our classification results we will use two different methods for segmentation.

The first method uses the active contour segmentation by Chan and Vese [2]. This algorithm detects objects in an image by starting a curve around objects and narrowing it down towards the objects. By stopping the curve the boundary of the objects is determined. Here, the following modifications proposed by Hoffmann [8] are applied: The contour to be found by the algorithm is set to a three dimensional function in order to evolve a three dimensional segmentation. The segmentation function is modified to achieve a smoother transition of the contour of the lesions which is defined by the newly introduced parameter α. This parameter regulates the smoothness of the level set function used by the segmentation by Chan and Vese. Last, the model is adapted to using all five images of a MRI time series, the pre-contrast and the four post-contrast images.

This allows more individual information to be given to the algorithm. Thus, if one image provides little information about where the boundary should lie, another image may provide more information which is used additionally. However, the quality of the resulting segmentation is strongly depending on the choice of the parameter α introduced by Hoffmann and the parameter μ of the original algorithm by Chan and Vese defining the length of the contour.

The second method we use to derive a segmentation is by ICA. The general idea of segmentation by ICA is that each independent component estimated by ICA contains a different tissue type. Other than the segmentation by Chan and Vese in its modification by Hoffmann it is possible to extract segmentations not only for the tumor curve, but for all extracted tissue types. In the end it has to be decided which component is seen as the main lesion component and can be used for the further workflow as segmentation containing the lesion. Segmentation by ICA is conducted in the following way: ICA has to be applied slice per slice, since the whole 3-dimensional cut out box around the lesion contains too many differently enhancing voxels. As the number of independent components is limited by the number of captured MR images, no clear independent components could be gained from an application of ICA on the whole box. To define the size of the region included in the segmentation, a threshold ρ has to be introduced, as for all segmentation algorithms. We define the threshold $\rho \in]0,1[$ so that voxels $v_{c_{ks}}$ of an independent component c_k and a slice s are contained in the segmentation if

$$si(v_{c_{ks}}) >= \rho \cdot \max si(v_C) \tag{1}$$

where $si(v_{c_{ks}})$ is the signal intensity of a voxel and $C = c_{is}$ is the matrix containing the independent components i for each slice s. This threshold takes into account that some lesion containing independent components show a higher maximum signal intensity values than others, which can be used for segmentation. To extract as much information as possible, we set the number of independent components to the maximum of 4. Next, the 4 independent components from every slice have to be matched in order to build a segmentation each including all slices. In order to fit each slice s_c of a independent component c to the corresponding next slice $(s+1)_c$ the similarities of the mixing matrices A_s and A_{s+1} are observed. Therefore, the difference matrix D is defined as

$$D = (d_{ij}) \quad with \quad d_{ij} = \sum_{k=1}^{|C|} |a_{s_{ki}} - a_{s+1_{kj}}| \tag{2}$$

where $|C|$ is the amount of independent components estimated, and $a_{s_{ki}}$ and $a_{s+1_{kj}}$ are elements of the matrices A_s resp. A_{s+1}. Matrix D now contains the sum of the absolute differences of every intensity of the enhancement curves of all independent components of slice s to slice $s+1$. Now the independent components are obtained as follows:

1. Find the indices i and j that minimize d_{ij}.
2. Map the $i-th$ independent component of slice s to the $j-th$ independent component of slice $s+1$.

3. Remove the $i-th$ row and the $j-th$ column from D.
4. Proceed with 1. if D non-empty.

By this method independent components that show similar enhancement curves are assumed to belong to the same tissue type. This is in accordance to the general idea of ICA on DCE. Since especially the tumor curve usually shows a much different enhancement curve than the other tissue curves, this method guarantees a good mapping for the lesion components with are most important for further calculations. On contrary mappings that use the similarity of the independent components itself have the disadvantage that usually lesion tissue grows or decreases from one slice to the other. Hence, a mapping based on these similarities is less successful. Also, independent components that show only slight and indifferent enhancement curves, which might cause bad mappings, usually containing noise, do show low overall signal intensities that are not included by the segmentation due to threshold ρ. Figure 4 presents the final segmentations by this method ($\rho = .35$) for the independent components 3 and 4 of the example of Figure 3.

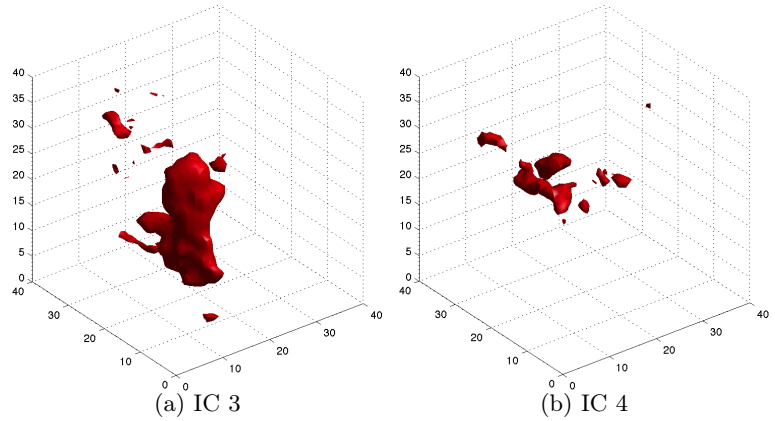

(a) IC 3 (b) IC 4

Fig. 4: Segmentation by ICA of ICs 3 and 4 of malignant MRI case.

Slice-wise ICA An alternative way to build a lesion segmentation is to apply ICA directly on the preprocessed data. After a whitening step for decorrelation and unit variance, the selected box around the lesion is processed slice per slice by ICA. We again choose to extract four independent components from each slice. Unlike for segmentation we do not choose a threshold to decide which voxels to include. All voxels of each slice are used to construct the enhancement curves. The resulting four enhancement curves of each slice have to be matched to the curves of the other slices, which is done following the matching algorithm described above. For comparison of the results in Section 4, parallel, our workflow also applies only whitening, but not ICA in this step.

Defining Characteristic Curve For feature extraction we need a mutual basis derived from the different segmentation methods and from slice-wise ICA. Thus, we define a characteristic curve for each MRI case. This curve is a single regular enhancement curve consisting of one pre-contrast and four post-contrast time points. It is derived from the different methods and is used to describe the lesion for feature extraction. For segmentation by Chan and Vese in the modification by Hoffmann it is simply calculated as the mean enhancement of all voxels of the subtraction images that are included in the segmentation. For segmentation by ICA it first has to be decided which segmentation relates to the lesion. Then, the characteristic curve is derived in the same way as described. For slice-wise ICA also the mean kinetic curve has proved to be most useful. Here, for each set of enhancement curves for each slice the mean of each pre- and post-contrast time point is calculated. Resulting in one curve for each independent component, the lesion component is chose as the strongest enhancing curve, i. e. showing the largest integral.

Feature Extraction and Selection As intermediate result every MRI case is represented by its characteristic kinetic curve. Now, we define features directly from curve parameters (features $\mathbf{f}_1$ to $\mathbf{f}_3$) or from parameters of curve approximating functions (features $\mathbf{f}_4$ to $\mathbf{f}_7$). These features will be selected for classification in the next step.

- $\mathbf{f}_1$, $\mathbf{f}_2$ and $\mathbf{f}_3$: Every characteristic curve consists of five points a_i for each time point $(i-1)\cdot \Delta t$ where $i \in \{1,..,5\}$ and $\Delta t = 1.4 \cdot 60s$ (as determined by the MRI protocol). Feature $\mathbf{f}_1 = (a_3 - a_2)/a_2$ considers the relation of growth or decline between the second and third time point to the initial growth to the second time point. Feature $\mathbf{f}_2 = (|a_3 - a_2| + |a_4 - a_3| + |a_5 - a_4|)/(a_2)$ widens the scope to the absolute values of growth or decline of all time points, again in the same relation. Feature $\mathbf{f}_3 = (a_5 - a_2)/a_2$ differs from $\mathbf{f}_2$ only in using the total growth or decline instead of absolute values.
- $\mathbf{f}_4$: Jansen et al. [10] has proposed a model for approximating tumor curves composed by two exponential functions: $y(t) = A \cdot \big(1 - \exp(-\alpha t)\big) \cdot \exp(-\beta t)$ with parameters A, α and β to be fitted. It expresses the early growth of the lesion curve as well as its latter decline or further growth. Apart from the fitted parameters feature vector $\mathbf{f}_4$ consists of Jansen's derived parameters except SER and the maximum value $y(t)$ reaches in the observed interval.
- $\mathbf{f}_5$ and $\mathbf{f}_6$: The model proposed by Gliozzi [4] is also composed of two exponential functions to approximate lesion enhancement. We use a normalized form as $y(t) = \exp(r \cdot t + \frac{1}{\beta} \cdot (a - r) \cdot (\exp(\beta t) - 1))$ with $r = \frac{\alpha}{beta}$ and include the fitted parameters α, β and a together with the maximum value $y(t)$ in the feature vector $\mathbf{f}_5$. Feature $\mathbf{f}_6$ differs only in using a modification by Hoffmann [7] which removes the outer exponential function.
- $\mathbf{f}_7$: The relative signal intensity enhancement [18] approximates the second to fifth time point of the characteristic curve to linear function $y(t) = at + b$. Only parameter a is used as feature and is derived as $\mathbf{f}_7 = ((t_3 + t_4 + t_5) \cdot (a_3 + a_4 + a_5) - 5 \cdot (t_3 a_3 + t_4 a_4 + t_5 a_5))/((t_3 + t_4 + t_5)^2 - 5(t_3^2 + t_4^2 + t_5^2))$.

Classification For classifying MRI cases into malignant or benign cases we input the acquired features $\mathbf{f}_1$ to $\mathbf{f}_7$ into a support vector machine (SVM). We train a soft margin SVM using for standard kernel functions [20,3] on a part of our MRI cases. We use the linear (kernel 1), polynomial (kernel 2), radial basis function (kernel 3) and sigmoid kernel (kernel 4). The resulting classifier predicts for each MRI case if it contains benign or malignant lesions. The kernel functions map then input feature space to a higher dimensional space in order to find a class separation there.

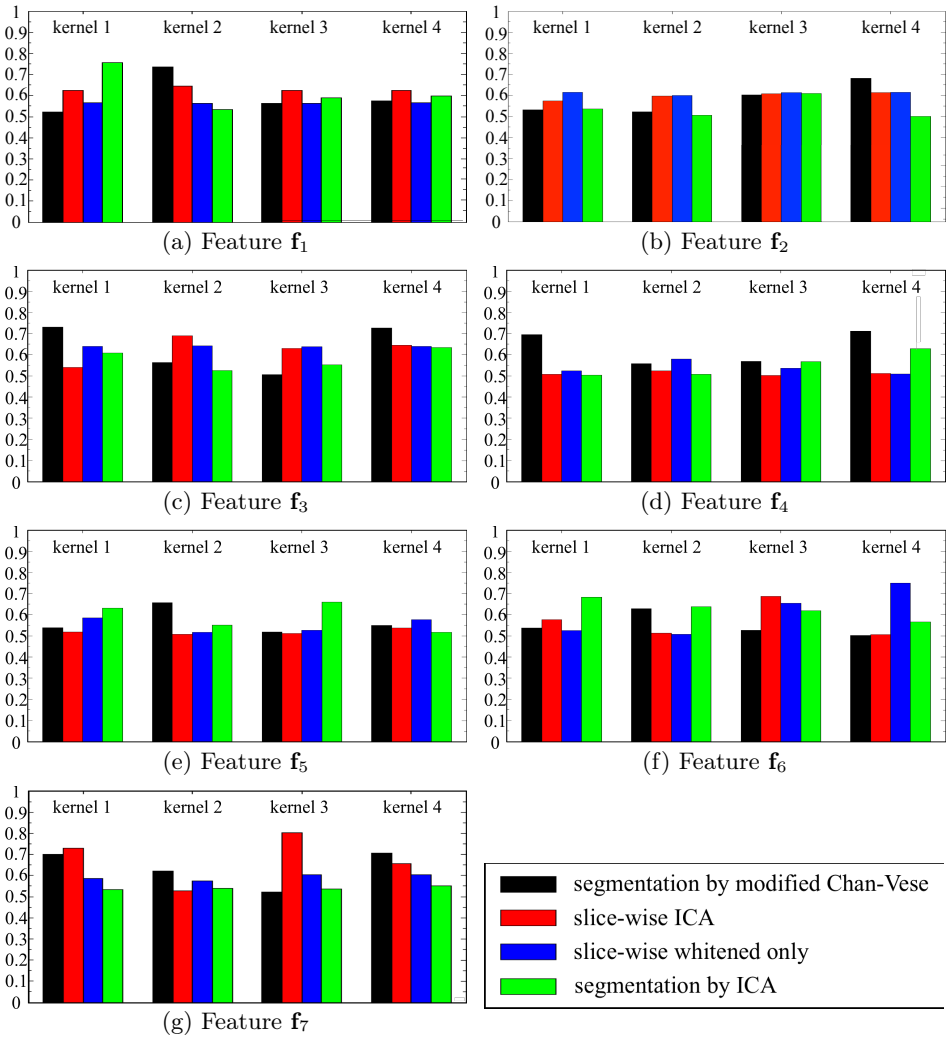

(a) Feature $\mathbf{f}_1$ (b) Feature $\mathbf{f}_2$

(c) Feature $\mathbf{f}_3$ (d) Feature $\mathbf{f}_4$

(e) Feature $\mathbf{f}_5$ (f) Feature $\mathbf{f}_6$

(g) Feature $\mathbf{f}_7$

Fig. 5: AUC of features 1 to 7.

4 Results and Discussion

To evaluate the surplus value of ICA we compare classification results from our workflow for segmentation by ICA and slice-wise ICA to the modified segmentation by Chan and Vese, and to the slice-wise only whitened data. As measure for quality of classification compare the area under the curve (AUC) as it is a standard measure for medical classification accuracy. The four kernels produce receiver operating characteristic (ROC) curves by the decision values obtained from the SVM. A high AUC values represents a good trade-off between sensitivity and specificity. $AUC = 1$ represents perfect classification with no false negatives or positives, $AUC = 0.5$ is equal to the random guess. The classifier for each feature is trained by n-fold cross validation. As source data serve 80 MRI cases recorded according to the MRI protocol of Table 1. The processed cases contain each one lesion, in total 57 malignant lesions and 23 benign lesions, mass-like and non-mass-like lesions as well. The values for the AUC of each feature and kernel as described in Section 3 are displayed in Figure 5. For the first feature that focuses on the begin of the enhancement curve the method using segmentation by ICA achieves the best AUC of .75 followed by the modified segmentation by Chan and Vese (Chan-Vese) with an AUC of .73. The second to fourth feature is still best classified when segmented by Chan-Vese. For the fifth feature again segmentation by ICA gains the best AUC of .66. For feature 6 slice-wise ICA reaches an AUC of .69, while the only whitened alternative results in an AUC of 0.75. Last and only for feature 7 an AUC of .80 is gained by ICA, while Chan-Vese comes only up to an AUC of .71. This feature combined with the method of slice-wise ICA clearly shows the benefit of using ICA.

5 Conclusion

We have shown that the application of ICA on DCE-MRI delivers good results for mass-like and non-mass-like lesions equally. As for non-mass-like lesions we outrun the ROI method by far. This certainly is due to the fact that ICA considers all existing lesion information. Automatic non-ICA-segmentation is also outrun in several features. ICA enables a very distinctive segmentation not only for lesion but also for other types of tissue or noise. Last, a fully parameter free automatic processing is given when using slice-wise ICA which delivers excellent results by an 80% AUC.

References

1. Brox, T., Bruhn, A., Weickert, J.: Variational Motion Segmentation with Level Sets. In: Computer Vision – ECCV 2006, pp. 471–483. Springer Berlin Heidelberg, Berlin, Heidelberg (Jan 2006)
2. Chan, T.F., Vese, L.A.: Active contours without edges. Image Processing, IEEE Transactions on 10(2), 266–277 (Feb 2001)
3. Cortes, C., Vapnik, V.: Support-Vector Networks. Machine Learning 20(3), 273–297 (1995)

4. Gliozzi, A.S., Mazzetti, S., Delsanto, P., Regge, D., Stasi, M.: Phenomenological universalities: a novel tool for the analysis of dynamic contrast enhancement in magnetic resonance imaging. Physics in Medicine and Biology 56, 573–586 (2011)
5. Goebl, S., Plant, C., Lobbes, M., Meyer-Baese, A.: Quantitative analysis of breast DCE-MR images based on ICA and an empirical model. In: Independent Component Analyses. p. 25. Ludwig-Maximilians-Univ. München (Germany) (May 2012)
6. Goebl, S., Plant, C., Lobbes, M., Meyer-Baese, A.: CAD-system based on kinetic analysis for non-mass-enhancing lesions in DCE-MRI. In: SPIE Defense, Security, and Sensing. p. 87500R. SPIE (May 2013)
7. Hoffmann, S.: Analysis of non-mass like tumors in breast MRI using methods of optical flow, segmentation and data mining. Master's Thesis, Saarland University (2011)
8. Hoffmann, S., Shutler, J.D., Lobbes, M., Burgeth, B., Meyer-Baese, A.: Automated analysis of non-mass-enhancing lesions in breast MRI based on morphological, kinetic, and spatio-temporal moments and joint segmentation-motion compensation technique. EURASIP J Adv Signal Process 2013(1), 172 (2013)
9. Hyvärinen, A., Oja, E.: Independent component analysis: algorithms and applications. Neural Networks 13, 411–430 (Jul 2000)
10. Jansen, S.A., Fan, X., Karczmar, G.S., Abe, H., Schmidt, R.A., Giger, M., Newstead, G.M.: DCEMRI of breast lesions: Is kinetic analysis equally effective for both mass and nonmass-like enhancement? Med. Phys. 35(7), 3102 (2008)
11. Jansen, S.A., Shimauchi, A., Zak, L., Fan, X., Karczmar, G.S., Newstead, G.M.: The diverse pathology and kinetics of mass, nonmass, and focus enhancement on MR imaging of the breast. Journal of Magnetic Resonance Imaging 33(6), 1382–1389 (May 2011)
12. Kaiser, W.A.: Signs in MR-Mammography. Springer (2009)
13. Koh, T.S., Thng, C.H., Ho, J.T.S., Tan, P.H., Rumpel, H., Khoo, J.B.K.: Independent component analysis of dynamic contrast-enhanced magnetic resonance images of breast carcinoma: A feasibility study. Journal of Magnetic Resonance Imaging 28(1), 271–277 (2008)
14. Liao, W., Chen, H., Huang, H., Mao, D., Yao, D., Zhao, X., Gao, J.: Spatial Independent Component Analysis for Multi-task Functional MRI Data Processing. International Journal of Magnetic Resonance Imaging 1(1), 49–60 (2007)
15. McKeown, M.J., Makeig, S., Brown, G.G., Jung, T.P., Kindermann, S.S., Bell, A.J., Sejnowski, T.J.: Analysis of fMRI Data by Blind Separation Into Independent Spatial Components. Human Brain Mapping 6, 160–188 (1998)
16. McKeown, M.J., Sejnowski, T.J.: Independent component analysis of fMRI data: Examining the assumptions. Human Brain Mapping 6(5-6), 368–372 (1998)
17. Newell, D., Nie, K., Chen, J.H., Hsu, C.C., Yu, H.J., Nalcioglu, O., Su, M.Y.: Selection of diagnostic features on breast MRI to differentiate between malignant and benign lesions using computer-aided diagnosis: differences in lesions presenting as mass and non-mass-like enhancement. Eur Radiol 20(4), 771–781 (Sep 2009)
18. Retter, F.: Improved Computer-Aided Diagnosis Scheme for Breast Lesions in DCE-MRI Based on Motion Artifact Removal and Integration of Morphologic and Dynamic Information. Master's thesis, Saarland University (2010)
19. Stoutjesdijk, M.J., Veltman, J., Huisman, H., Karssemeijer, N., Barentsz, J.O., Blickman, J.G., Boetes, C.: Automated analysis of contrast enhancement in breast MRI lesions using mean shift clustering for ROI selection. Journal of Magnetic Resonance Imaging 26(3), 606–614 (2007)
20. Vapnik, V., Lerner, A.: Pattern Recognition using Generalized Portrait Method. Automation and Remote Control 24 (1963)